

Restraint of angiogenesis by zinc finger transcription factor CTCF-dependent chromatin insulation

Ming Tang^a, Bo Chen^{b,c}, Tong Lin^a, Zhaozhong Li^a, Carolina Pardo^a, Christine Pampo^d, Jing Chen^e, Ching-Ling Lien^f, Lizi Wu^g, Lingbao Ai^a, Heiman Wang^a, Kai Yao^c, S. Paul Oh^h, Edward Setoⁱ, Lois E. H. Smith^e, Dietmar W. Siemann^d, Michael P. Kladde^a, Constance L. Cepko^b, and Jianrong Lu^{a,1}

^aDepartment of Biochemistry and Molecular Biology, ^dDepartment of Radiation Oncology, ^gDepartment of Molecular Genetics and Microbiology, ^hDepartment of Physiology and Functional Genomics, University of Florida College of Medicine, Gainesville, FL 32610-3633; ^bDepartment of Genetics and Howard Hughes Medical Institute, Harvard Medical School, Boston, MA 02115; ^cDepartment of Ophthalmology and Visual Science, Yale University School of Medicine, New Haven, CT 06511; ^eDepartment of Ophthalmology, Harvard Medical School, Children's Hospital Boston, Boston, MA 02115; ^fDepartment of Surgery, Keck School of Medicine, University of Southern California and The Saban Research Institute, Children's Hospital Los Angeles, Los Angeles, CA 90027; and ⁱDepartment of Molecular Oncology, H. Lee Moffitt Cancer Center and Research Institute, Tampa, FL 33612

Edited* by Eric N. Olson, University of Texas Southwestern, Dallas, TX, and approved August 16, 2011 (received for review March 28, 2011)

Angiogenesis is meticulously controlled by a fine balance between positive and negative regulatory activities. Vascular endothelial growth factor (VEGF) is a predominant angiogenic factor and its dosage is precisely regulated during normal vascular formation. In cancer, VEGF is commonly overproduced, resulting in abnormal neovascularization. VEGF is induced in response to various stimuli including hypoxia; however, very little is known about the mechanisms that confine its induction to ensure proper angiogenesis. Chromatin insulation is a key transcription mechanism that prevents promiscuous gene activation by interfering with the action of enhancers. Here we show that the chromatin insulator-binding factor CTCF binds to the proximal promoter of *VEGF*. Consistent with the enhancer-blocking mode of chromatin insulators, CTCF has little effect on basal expression of *VEGF* but specifically affects its activation by enhancers. CTCF knockdown cells are sensitized for induction of *VEGF* and exhibit elevated proangiogenic potential. Cancer-derived CTCF missense mutants are mostly defective in blocking enhancers at the *VEGF* locus. Moreover, during mouse retinal development, depletion of CTCF causes excess angiogenesis. Therefore, CTCF-mediated chromatin insulation acts as a crucial safeguard against hyperactivation of angiogenesis.

Nearly all tissues develop vascular networks that supply cells with nutrients and oxygen. Vascular development is a fundamental biological process that is tightly controlled by both pro- and antiangiogenic mechanisms (1). Physiological angiogenesis occurs primarily during embryogenesis and is active in the adult only under specific settings, such as during wound healing and in the female reproductive system (2). Under pathological conditions, angiogenesis can be aberrantly activated when the angiogenic balance tilts toward a proangiogenic direction. Excess angiogenesis contributes to a variety of vascular diseases, including cancer and pathological neovascularization in the retina.

At the heart of vascular development is the vascular endothelial growth factor (VEGF), a potent endothelial mitogen (3). VEGF is probably the most important stimulator of normal and pathological blood vessel growth. Primarily acting as a paracrine signal, VEGF promotes endothelial cell proliferation, survival, migration, vessel sprouting, and tube formation. VEGF also mobilizes and recruits bone marrow-derived endothelial progenitor cells into the nascent vasculature. Importantly, the effect of VEGF is dose dependent. A precise dosage of VEGF is critical for normal vascular development. During mouse embryogenesis, loss of even a single allele of *VEGF* results in early embryonic lethality due to severe vascular defects (4, 5). Conversely, excessive VEGF causes pathological angiogenesis. Therapeutic targeting of VEGF effectively inhibits angiogenesis and has been applied in clinical treatment of cancer and ocular diseases (3, 6).

VEGF expression is dynamically regulated by a variety of stimuli. Hypoxia is the principal driver of VEGF induction in both physiological and pathological angiogenesis (7, 8). Under

hypoxia, the hypoxia-inducible transcription factor (HIF) is stabilized and directly binds to the *VEGF* promoter to activate its transcription (7, 8). Several growth factors, cytokines, hormones, and oncoproteins induce VEGF as well (9, 10). The female steroid hormone estrogen regulates endometrial angiogenesis during the estrous cycle. Estrogenic induction of VEGF and angiogenesis is also an important facet of breast cancer development (11). However, it remains largely elusive how the induction of VEGF is appropriately confined for physiological angiogenesis and dysregulated under pathological conditions.

Many proangiogenic stimuli directly or indirectly activate *VEGF* transcription through enhancer elements at the *VEGF* locus. Eukaryotic gene regulation occurs in the context of chromatin. In addition to enhancers, chromatin insulators are among the key players in transcription (12–14). Insulators are regulatory DNA elements that interact with each other and/or with other nuclear structures to organize chromatin architecture. Insulators interfere with effective communication between promoters and enhancers when positioned between them, thereby preventing enhancers from promiscuously activating promoters. In vertebrates, such enhancer-blocking activity of insulators is mainly dependent on CTCF, a highly conserved zinc finger transcription factor (13).

In the present study, we identified a CTCF-bound insulator in the promoter of *VEGF*. CTCF restricts upstream enhancers from activating *VEGF*, thereby restraining induction of VEGF and angiogenesis. The enhancer-blocking function of CTCF at the *VEGF* gene appears to be lost or impaired in some cancer cells. Furthermore, during mouse retinal development, depletion of CTCF results in excess angiogenesis *in vivo*. Therefore, CTCF-dependent chromatin insulation plays a pivotal role in governing physiological vascular growth.

Results

Binding of CTCF to the *VEGF* Promoter. Under hypoxia, the HIF transcription factor activates *VEGF* transcription through the hypoxia responsive element (HRE) in the *VEGF* promoter. During our previous study on regulation of hypoxia-inducible genes (15), we noticed that reporters driven by the HRE-containing *VEGF* promoter responded poorly to hypoxic induction. This

Author contributions: J.L. designed research; M.T., B.C., T.L., Z.L., C. Pardo, C. Pampo, L.A., H.W., K.Y., and J.L. performed research; C.-L.L., L.W., S.P.O., E.S., D.W.S., M.P.K., and C.L.C. contributed new reagents/analytic tools; M.T., B.C., T.L., Z.L., C. Pardo, J.C., L.E.H.S., M.P.K., C.L.C., and J.L. analyzed data; and J.L. wrote the paper.

The authors declare no conflict of interest.

*This Direct Submission article had a prearranged editor.

¹To whom correspondence should be addressed. E-mail: jrlu@ufl.edu.

This article contains supporting information online at www.pnas.org/lookup/suppl/doi:10.1073/pnas.1104662108/-DCSupplemental.

observation prompted us to search for potential mechanisms that counteract transcriptional activation, such as enhancer-blocking chromatin insulation. CTCF is the only known enhancer-blocking factor in mammals. The HRE is located about 1 kb upstream of the transcription start site (TSS) of *VEGF*. Analysis of the DNA sequence between the HRE and TSS with an in silico CTCF binding prediction program (16) identified a putative CTCF consensus binding site, which is located about 600 bp upstream of the TSS and highly conserved in mammals (Fig. S1).

To test whether CTCF indeed recognized this motif at the *VEGF* promoter, in vitro electrophoretic mobility shift assay (EMSA) was performed. A small DNA fragment from the *VEGF* proximal promoter carrying the CTCF-binding motif was labeled and incubated with purified CTCF proteins. Formation of a CTCF–DNA complex was detected, which was supershifted by an anti-CTCF antibody (Fig. 1A), confirming that CTCF directly bound to this fragment.

We next carried out chromatin immunoprecipitation (ChIP) analysis to validate the binding of CTCF to the *VEGF* promoter in intact MCF7 breast cancer cells. Strong occupancy of CTCF at the proximal promoter of *VEGF* was observed (Fig. 1B). Binding of CTCF to *VEGF* was also observed in various human cell lines (Fig. S2). Recently, the cohesin complex was shown to colocalize with CTCF in the genome and contribute to CTCF's chromatin insulation activity (17–20). We investigated the presence of cohesin at the *VEGF* locus in MCF7 cells. ChIP assay with antibodies against Rad21 (also known as SCC1, a subunit of cohesin) revealed that cohesin and CTCF overlapped at the *VEGF* proximal promoter region (Fig. 1C).

Enhancer-Blocking Activity of CTCF at the *VEGF* Promoter. CTCF has been reported to act as a transcriptional activator, repressor, or insulating factor, depending on the context. We were interested in characterizing the significance of the CTCF-binding site at the *VEGF* promoter in transcription of *VEGF*. In the *VEGF* 5' region, the CTCF site is located between the HRE and the TSS (Fig. 2A), a setting reminiscent of enhancer blocking. Therefore, we examined possible enhancer blocking using previously established episomal reporter-based assays (21). Two copies of HRE from the *VEGF* gene, serving as an enhancer, were placed in front of a luciferase reporter with a basal promoter. Then the CTCF-binding site was inserted either upstream of the HREs or between the HREs and the basal promoter. HEK293 cells were transiently transfected with linearized reporter constructs and subjected to treatment with the hypoxia mimetic dipyrindyl (DP), which stabilizes HIF by chelating iron. This treatment potentially

activated the HRE-only reporter by 50-fold (Fig. 2B). When the CTCF site was placed outside the HREs, the hypoxic induction was only slightly reduced (Fig. 2B), implying that this element did not act as a strong silencer. However, when the CTCF-binding element was placed between the HREs and the basal promoter, a drastic decrease in reporter induction was observed (Fig. 2B). This mode of transcriptional regulation is characteristic of the defined chromatin insulator properties. Therefore, the CTCF binding site from the *VEGF* promoter behaved like a classic enhancer blocker, interfering strongly with enhancer action in a position-dependent manner.

We asked whether this CTCF site was capable of blocking the action of other enhancers. Estrogens stimulate transcription of *VEGF*, although the underlying regulation remains unclear (11). Recent genome-wide ChIP assays uncovered multiple binding regions of the estrogen receptor ER α around the *VEGF* locus, including –56 kb, –46 kb, –10 kb upstream, and +34 kb downstream of the TSS (Fig. 2A) (22, 23). We identified putative estrogen responsive elements (EREs) from these regions and linked them individually to a luciferase reporter. These reporters were cotransfected with ER α into HEK293 cells and tested for estrogen induction. Single copy of each ERE from the –56 kb, –46 kb, and –10 kb upstream regions conferred mild induction of the reporter gene activity in response to estrogen treatment, and two copies of each ERE demonstrated more robust responses (Fig. S3). The latter was then used in enhancer-blocking assays. As expected, the same CTCF binding site strongly reduced the activity of the reporter induced by estrogen when it was located between the EREs and the promoter (Fig. 2C).

Using RNA interference to knock down CTCF, we determined whether the enhancer-blocking activity of this DNA fragment was indeed attributable to CTCF. HEK293 cells were first transduced with lentivirus expressing either control or CTCF short-hairpin RNA (shRNA). These cells were then transfected with HRE-driven reporters carrying the CTCF binding site between the promoter and HREs and subsequently treated with DP. Depletion of CTCF enhanced induction of reporter activity (Fig. 2D), suggesting down-regulation of CTCF, at least partially relieved enhancer blocking by the CTCF binding site. Therefore, CTCF is responsible for the enhancer-blocking activity mediated by the CTCF binding site from the *VEGF* promoter.

CTCF Constrains Transcriptional Induction of the Endogenous *VEGF* Promoter. Although reporter-based assays have widely been used to identify enhancer blockers in fly and vertebrate cells, the more critical test is whether CTCF exerts chromatin insulation activity

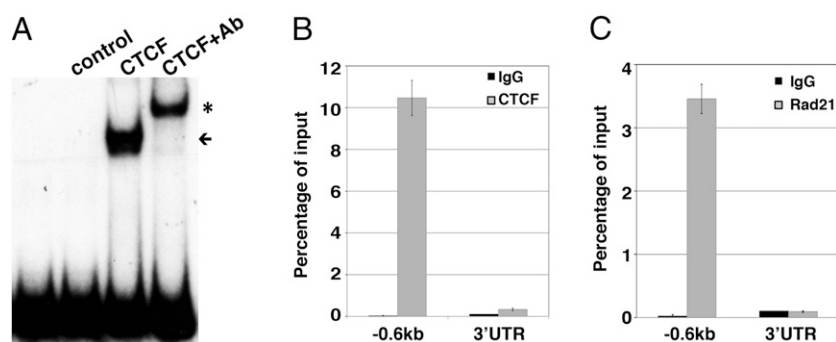


Fig. 1. Binding of CTCF to the *VEGF* promoter. (A) EMSA analysis of CTCF binding to the *VEGF* promoter in vitro. A radiolabeled 100-bp DNA fragment carrying the CTCF-binding site from the *VEGF* promoter was incubated with control lysate or purified CTCF protein, and the mixture was separated by native polyacrylamide gel electrophoresis. Arrow indicates the DNA–CTCF complex; * denotes the supershifted complex by an anti-CTCF antibody. (B) ChIP analysis of CTCF binding at the *VEGF* proximal promoter. MCF7 cells were cross-linked and sonicated. Sonicated chromatin fragments were precipitated with an anti-CTCF antibody or control IgG. The relative concentrations of DNA fragments at the *VEGF* locus in the immunoprecipitated fractions were determined by real-time quantitative PCR. The 3'–UTR served as a reference sequence. (C) ChIP analysis of cohesin occupancy at the *VEGF* locus with an anti-Rad21 antibody. The assay was performed similarly to B.

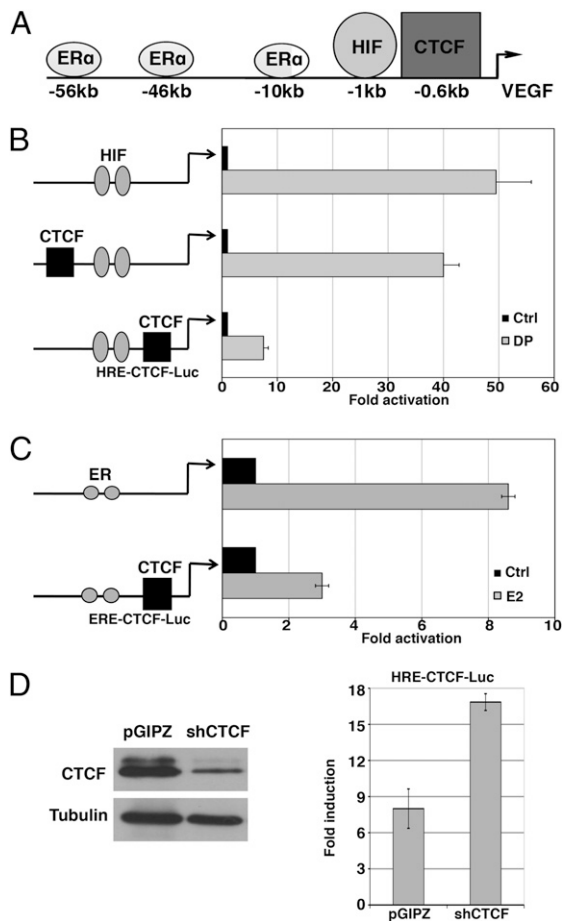


Fig. 2. Enhancer-blocking activity of CTCF in reporter-based assays. The CTCF site from the *VEGF* promoter was tested in different positions relative to enhancers (i.e., HRE and ERE) in various luciferase constructs. Before transfection, all constructs were linearized to avoid bidirectional action of the enhancers due to the circular nature of plasmids. (A) Schematic organization of the 5' region of the *VEGF* gene. The binding sites for ER α , HIF, and CTCF are shown. (B) CTCF blocks HRE function. The scheme of each reporter construct with the HREs and the CTCF site is shown at the *Left* of the histogram. HEK293 cells were transiently transfected and 1 d later, treated with DP (100 μ M). Luciferase assay was performed 2 d after transfection. Histogram shows relative luciferase reporter activities. (C) CTCF blocks ERE function. The reporter constructs with EREs and the CTCF site are shown schematically. Similar to *B*, 1 d after transfection, HEK293 cells were treated with E2 (100 nM), and luciferase activities were determined the following day. (D) Enhancer-blocking activity is attributable to CTCF. HEK293 cells were transduced with lentiviral vector (pGIPZ) or shRNA targeting CTCF (shCTCF). The knockdown efficiency of CTCF was determined by immunoblotting (*Left* of the histogram). Subsequently, the transduced cells were transiently transfected with luciferase reporters. DP treatment and luciferase assay were carried out similarly to *B*.

at the endogenous *VEGF* locus. We knocked down CTCF in ER α ⁺ MCF7 cells using shRNA and monitored expression of endogenous VEGF after treating the cells with DP or estrogen. CTCF knockdown did not increase the expression levels of the VEGF activators HIF and ER α (Fig. S4). On the basis of Northern blotting analysis, depletion of CTCF alone did not result in notable activation of VEGF (Fig. 3A, lanes 3 and 4), consistent with the model that CTCF does not primarily function as a transcriptional silencer at the *VEGF* locus. Upon estrogen treatment, the control cells showed modest induction of VEGF (Fig. 3A, lanes 1 and 3); however, this induction became much more robust in CTCF-depleted cells (Fig. 3A, lanes 1 and 2). Similarly, DP stimulation resulted in higher VEGF expression in the CTCF-depleted cells

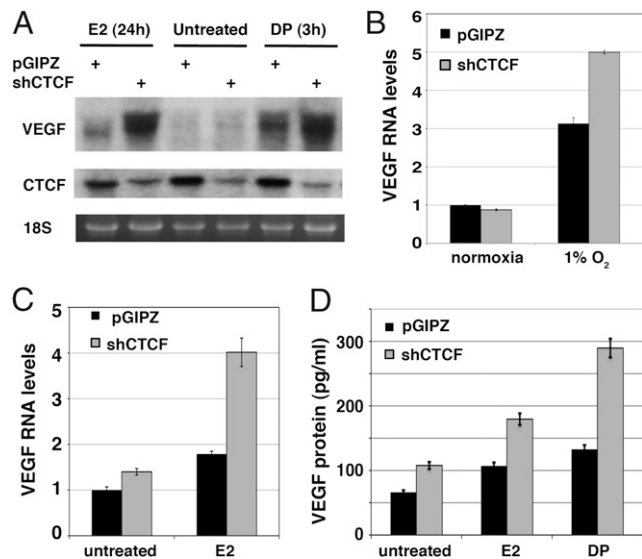


Fig. 3. CTCF restrains the induction of endogenous VEGF and angiogenesis. (A) Northern blotting analysis of VEGF and CTCF in vector control (pGIPZ) and CTCF-depleted MCF7 cells under estrogen E2 (100 nM) and DP (100 μ M) treatment for indicated time. Ribosomal RNA (18S) served as a loading control. (B and C) Quantitative measurement of VEGF RNA levels in pGIPZ control and CTCF-depleted cells under hypoxia (1% O₂) and estrogen treatments, respectively. (D) VEGF protein concentrations in conditioned media from pGIPZ control and CTCF-depleted MCF7 cells after 24-h treatment with DP or estrogen. The assay was performed with a VEGF ELISA kit (Invitrogen) following the manufacturer's instructions.

than in the control cells (Fig. 3A, lanes 5 and 6). Elevated hypoxic induction of VEGF due to depletion of CTCF was also observed in MDA-MB-435 cancer cells (Fig. S5). These results are consistent with the enhancer-blocking role of CTCF at the *VEGF* gene.

We also placed the cells under low O₂ tension (1%) and determined VEGF expression by quantitative real-time RT-PCR. Similar to stimulation by estrogen and DP, induction of VEGF by hypoxia was stronger in the CTCF-depleted cells than that in the control cells (Fig. 3B). For comparison, we examined the expression pattern of several hypoxia-inducible genes including PGK1, LDHA, and PDK1, which are not targets of CTCF, and found that their induction by hypoxia was not augmented by depletion of CTCF (Fig. S6). Thus, the enhancer-blocking effect of CTCF is not general to all hypoxia-inducible genes, but rather specific to the *VEGF* gene.

Expression of VEGF RNA in response to estrogen in control vs. CTCF-depleted cells was also confirmed by quantitative measurement (Fig. 3C). In addition, we quantified the protein concentrations of VEGF in the conditioned media from the control and CTCF-depleted MCF7 cells under DP and estrogen treatment (Fig. 3D and Fig. S7). CTCF-depleted cells secreted higher levels of VEGF protein than the control cells upon stimulation. These observations suggest that CTCF acts as an enhancer blocker to ensure appropriately confined VEGF induction.

Negative Regulation of Tumor Angiogenesis by CTCF. If CTCF-depleted cells produced more VEGF in response to angiogenic stimuli, these cells would be predicted to be more proangiogenic. We assessed angiogenic potential by assaying *in vitro* tube formation of endothelial cells (ECs) on a Matrigel substrate. Conditioned media from CTCF-depleted MCF7 cells exhibited more potent angiogenic activity than those from control cells (Figs. S8 and S9).

We extended this study with an *in vivo* intradermal angiogenesis assay (24). Control or CTCF-depleted MCF7 cells were

injected intradermally into immunodeficient mice to test whether CTCF depletion led to increased vessel sprouting from the existing host vasculature. Two days after injection, the number of new blood vessels induced by tumor cells was counted. CTCF-depleted tumor cells induced more capillaries than the corresponding control cells (Fig. 4A, untreated). Feeding mice with estrogen increased capillary vessel density by the control cells, and this effect was further enhanced by knockdown of CTCF (Fig. 4A, E2). Therefore, CTCF limited the angiogenic potential of tumor cells *in vivo*.

Because abnormal proliferative vascularization is nearly universal in cancer, we suspected that CTCF-mediated restriction of angiogenesis might be impaired in cancer. Four distinct somatic missense mutations of CTCF were previously identified in breast, prostate, and Wilms' tumors (25). CTCF is a multivalent transcription factor and uses different combinations of zinc fingers (ZFs) to bind diverse target sequences (14). Tumor-derived point mutations in ZF3 and ZF7 did not totally abrogate the DNA-binding ability of CTCF; instead, they selectively blocked binding to some CTCF target sites, but not to others (25).

We first tested whether the tumor-specific CTCF mutants were able to bind to the *VEGF* promoter. Flag-tagged wild-type and four mutant full-length CTCF proteins were expressed in HEK293 cells, purified with anti-Flag antibodies, and analyzed for binding to the insulator element from the *VEGF* promoter by EMSA. ZF3 mutants H345R and R339W showed dramatically diminished binding (Fig. 4B, lanes 3 and 4). By contrast, like wild-type CTCF, the ZF3 mutant K344E and ZF7 mutant R448Q retained high levels of DNA binding (Fig. 4B, lanes 1, 2, and 5). On the basis of zinc finger domain structure, R339 is in the DNA recognition domain and is critical for direct interaction with DNA, whereas H345 binds zinc and maintains the ZF structure. Mutations in R339 and H345, but not K344, are hence expected to disrupt DNA binding. Thus, ZF3 is essential for CTCF to bind to the *VEGF* promoter. R448 is also located in a DNA-recognition position, indicating that ZF7 is not involved in *VEGF* binding.

We then examined the enhancer-blocking activity of the tumor-derived CTCF mutants on VEGF induction. MCF7 cells were depleted of endogenous CTCF by lentiviral shRNA and subsequently transduced with lentiviruses expressing wild-type or tumor-derived mutant CTCF cDNAs. These cDNAs were modified to be resistant to shRNA targeting CTCF. Efficient depletion of endogenous CTCF and replacement expression with exogenous wild-type or tumor mutant CTCF proteins was verified by Western blotting (Fig. S10). The reconstituted cells were

subjected to hypoxic induction with DP and the RNA levels of VEGF were determined quantitatively. In response to stimulation, cells reconstituted with the ZF7 R448Q mutant CTCF displayed similar VEGF induction to cells reconstituted with wild-type CTCF (Fig. 4C), suggesting CTCF ZF7 is dispensable for enhancer-blocking activity at *VEGF*. However, cells reconstituted with each of the three ZF3 mutants showed increased induction of VEGF (Fig. 4C), a pattern observed in CTCF-deficient cells (Fig. 3B). This finding suggests that tumor-derived CTCF ZF3 mutant proteins are defective in enhancer blocking of VEGF in cells. Unlike H345R and R339W that interrupted the binding of CTCF to *VEGF*, the K344E substitution possibly disrupted recruitment of CTCF cofactors essential for enhancer blocking. The results imply that tumors with CTCF mutations may gain abnormally elevated angiogenic potential.

Requirement of CTCF in Physiological Angiogenesis of the Retina.

Angiogenesis is vital to normal retinal development. Pathological neovascularization in the retina is the leading cause of blindness (26). Because CTCF regulated VEGF induction and tumor angiogenesis, we were interested in defining its role in physiological vascular development in the eye.

The mouse retina is an intricately organized, striated tissue with distinct neuronal and vascular layers. Expression of VEGF, a key angiogenic stimulus in the developing retina, is activated by cellular oxygen tension (physiological hypoxia) (27). In mouse, the retinal vasculature develops postnatally (26). The superficial vascular plexus forms within the ganglion cell layer (GCL) during the first week after birth. From postnatal day 7 (P7), the planar superficial plexus branches perpendicularly, forming first the deep and then the intermediate vascular plexuses at the outer and inner edges of the inner nuclear layer (INL), respectively. Notably, the photoreceptor-containing outer nuclear layer (ONL) completely lacks blood vessels.

To investigate the function of CTCF in retinal angiogenesis *in vivo*, plasmids expressing green fluorescent protein (GFP) together with control or CTCF shRNA were directly injected into the subretinal space of neonatal (P0) mouse pups, followed by electroporation (28). Electroporated retinas were harvested and analyzed at P14. GFP signal in cross-section was detected in the ONL and its outer segments, INL, and axons and vascular plexus between the GCL and INL (Fig. S11), suggesting that these cells were efficiently transfected. The control shRNA-transfected retina maintained its appropriately organized architecture without obvious vascular abnormalities (Fig. 5). By con-

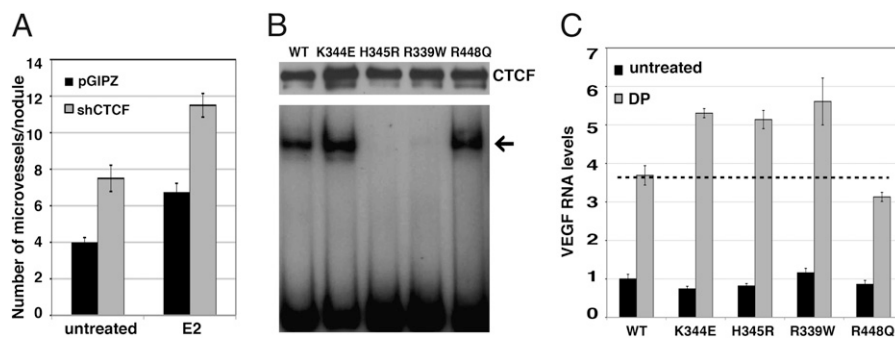


Fig. 4. CTCF negatively regulates tumor angiogenesis. (A) Intradermal angiogenesis assay of pGIPZ control and CTCF-depleted MCF7 cells. Mice were s.c. inoculated with control or shCTCF MCF7 cells. Half of the mice were daily fed with estrogen (E2). Two days later, tumor nodules were collected and microvessels around each tumor were counted. The number of capillary vessels per tumor nodule was shown ($n = 4$ per group). Error bars represent SD. (B) EMSA analysis of the binding activity of cancer-derived CTCF mutants to the *VEGF* promoter. Flag-tagged wild-type (WT) and various mutant CTCF proteins were immunoprecipitated from HEK293 cells with anti-Flag antibodies. These proteins were eluted and subjected to EMSA. The loading of CTCF proteins used in EMSA is shown at the *Top*. Arrow indicates the DNA–CTCF complexes. (C) Cancer-derived CTCF mutants are deficient in enhancer blocking of VEGF. MCF7 cells were first depleted of endogenous CTCF and subsequently transduced with lentivirus expressing exogenous WT and mutant CTCFs. Reconstituted cells were treated with DP, and VEGF transcript levels were determined by quantitative RT-PCR.

trast, in the CTCF shRNA-electroporated retina, there was a higher density of blood vessels, especially in the deep vascular plexus and “vertical” capillary sprouts (Fig. 5). The vascular phenotype was observed specifically in areas transfected with shRNA targeting CTCF (Fig. S11). Vessels in the affected area appeared to be irregularly shaped and chaotically orientated. The vertical vasculature apparently was guided along tracks of GFP⁺ cells (possibly Müller glial cells) (Fig. 5). More dramatically, it was evident that ectopic capillary vessels sprouted from the deep plexus and invaded the normally avascular ONL (Fig. 5). The vascular penetration into ONL demonstrated ectopic angiogenesis. This phenotype partially resembles neovascularization observed in transgenic mice with retinal overexpression of VEGF, in which vascular branches originating from the deep plexus extended into the photoreceptor layer (29). Taken together, the results demonstrate that CTCF governs normal vascular formation in the developing retina, and depletion of CTCF causes excess intraretinal neovascularization.

Discussion

Understanding the biological principles that direct vascular growth has important clinical implications. As a crucial driver for both physiological and pathological angiogenesis, the levels of VEGF are under tight control. Here we show there exists a CTCF-dependent chromatin insulator element at the proximal promoter region of the *VEGF* gene. Binding of CTCF interferes with activation of VEGF by its enhancers, thereby restraining induction of VEGF in response to proangiogenic stimuli. CTCF deficiency leads to excess angiogenesis in vivo. Our study identifies CTCF-dependent chromatin insulation as a critical mechanism to prevent VEGF from overproduction and assure proper vascular formation.

Chromatin insulation represents a unique transcription mechanism. However, other than the best-understood imprinted *Igf2/H19* locus, very few mammalian enhancer-blocking insulators have been well characterized. Insulators do not directly activate or repress basal gene expression, but exert their activity by counteracting enhancers. The action of insulators is not absolute, but rather quantitative (30). Insulation depends on the strength of enhancers. An insulator may effectively block a weak enhancer, but may be overwhelmed by a potent enhancer (30). In the case of VEGF, the CTCF-bound insulator exhibited a stronger effect in impeding estrogen than hypoxia (Fig. 3), which is consistent with the fact that HIF is a more potent transcription activator than ER α . CTCF-dependent insulation at *VEGF* may

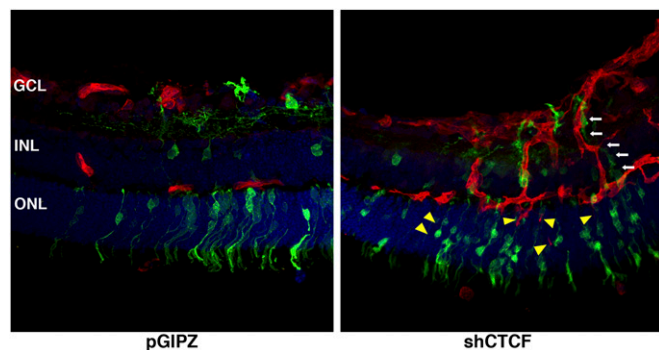


Fig. 5. Depletion of CTCF causes abnormal angiogenesis in the developing retina. Neonatal mouse retinas were subjected to subretinal injection of shRNA plasmids (pGIPZ control or shCTCF) followed by electroporation. Cross-sections of P14 retina are shown. Endothelial cells were selectively stained with isolectin B4-Alexa 594 (red) and nuclei with DAPI (blue). Ectopic growth of blood vessels into the photoreceptor layer is indicated by arrowheads. “Vertical” vessels migrated along GFP⁺ track (arrows).

not only prevent illegitimate activation by transient, randomly fluctuating signals, but also control the magnitude of VEGF induction. Therefore, chromatin insulation offers a dosage-control mechanism, which is particularly critical for angiogenesis.

Cancers are typically highly vascularized. This phenotype may result from intratumoral hypoxia (a hallmark of rapidly growing solid tumors), oncogenic signaling, and, in some cases, defects in CTCF. The CTCF-dependent dosage control of VEGF is likely to be impaired/lost in cancer. It was reported that CTCF expression was significantly reduced in lobular carcinoma in situ (LCIS) of the breast compared with normal parenchymal cells (31), and CTCF levels inversely correlated with breast tumor histological grades (32). CTCF is also mutated somatically in several types of cancers (25). CTCF is located on human chromosome 16q22, which frequently undergoes loss of heterozygosity (LOH) in breast and prostate cancers (33). In tumors harboring missense CTCF mutations, the normal CTCF allele was lost (25). We have shown that three out of four tumor-derived CTCF mutants are deficient in enhancer blocking at the *VEGF* locus. Furthermore, it is possible that the CTCF site at the *VEGF* promoter might be methylated in cancer cells, which might block CTCF binding. Together, CTCF’s insulation activity at *VEGF* may be compromised in advanced cancer, conferring tumor cells with increased induction of VEGF (e.g., in response to tumor hypoxia), hence augmented angiogenic potential and selective growth advantage.

Materials and Methods

Plasmids, Cells, Antibodies, and Chemicals. CTCF and VEGF cDNAs and shRNA plasmids were obtained from OpenBiosystems. Luciferase reporter constructs were generated by cloning the indicated DNA elements into pGL3-promoter (Promega). Human cell lines HEK293, MCF7, HCT116, MDA-MB-231 and -435 were cultured in Dulbecco’s modified eagle medium (DMEM) containing 10% bovine calf serum (Gibco). Murine pulmonary ECs were cultured in endothelial cell medium (ECM) in which DMEM (Gibco) was supplemented with 20% FBS (HyClone), 0.5% heparin (200 mg/mL; Sigma), 1% endothelial mitogen (10 mg/mL; Biomedical Technologies), 1% nonessential amino acids (Mediatech), 1% sodium pyruvate (100 mM; Invitrogen), and 0.4% penicillin-streptomycin (Invitrogen). All culture plates (Falcon) and flasks (Falcon) used for the EC culture were coated with 1:5 diluted bovine fibronectin stabilized solution (1 mg/mL; Biomedical Technologies) and then incubated at 37 °C for 30 min before each use. Antibodies for CTCF were purchased from Millipore (no. 07-729) and Cell Signaling (no. 3418), anti-Rad21 from Abcam (no. ab992), antitubulin from Sigma (no. T6199), anti-HIF1 α from BD Biosciences (no. 610958), and anti-ER α from Santa Cruz (no. sc-543). Chemicals dipyrindyl and estrogen E2 were obtained from Sigma.

ChIP Analysis. ChIP assay was conducted as previously reported (34). Briefly, cells were cross-linked with 1% formaldehyde for 10 min. The reaction was stopped by the addition of glycine. Cross-linked cells were washed in 1 \times PBS and collected. Cell pellets were washed with washing buffer (0.25% Triton X-100, 10 mM ethylene diamine tetraacetic acid (EDTA), 0.5 mM ethylene glycol tetraacetic acid (EGTA), 10 mM Tris pH 8.0), resuspended in sonication buffer (1 mM EDTA, 0.5 mM EGTA, and 10 mM Tris pH 8.0), mixed with glass beads, and subjected to sonication. The sonicated samples were diluted in ChIP buffer (0.01% SDS 1.0% Triton X-100, 1.0 mM EDTA, 20 mM Tris pH 8.1, 150 mM NaCl) and incubated with antibodies (for CTCF and Rad21) and protein A slurry (Invitrogen). The immunoprecipitates were subjected to a series of washing steps to remove nonspecific binding material. After reversal of cross-linking, DNA samples were purified and the enrichment of specific genomic regions was determined by real-time quantitative PCR. Final results represent percentage of input chromatin and error bars indicate SD from triplicate experiments.

Northern Blotting, Western Blotting, EMSA, RT-PCR, and Luciferase Assays.

Northern blotting, Western blotting, and EMSA were carried out following standard molecular biology protocols. For Northern blotting, total RNA from cells was extracted with TRIzol reagent (Invitrogen), and cDNA fragments of CTCF and VEGF were ³²P-radiolabeled and used as probes. Reverse transcription of RNA was conducted using Moloney murine leukemia virus (M-MuLV) reverse transcriptase with random primers. The expression levels of selected genes were determined by real-time PCR. Data were normalized

against β -actin. For luciferase assays, HEK293 cells were transiently transfected with various firefly luciferase constructs and an SV40-driven Renilla luciferase reporter. The latter was included to normalize transfection efficiency. Experiments were performed in duplicate. Data points represent the mean value \pm SD.

CTCF Reconstitution Assay. MCF7 cells were infected with lentivirus expressing shRNA targeting CTCF. After selection with puromycin (1 μ g/mL) for 1 wk, knockdown efficiency was verified by immunoblotting with anti-CTCF antibodies. These cells were then transduced with lentivirus expressing GFP and wild-type or cancer-derived mutant CTCF cDNAs, all of which were made resistant to shRNA knockdown by introduction of silent mutations. Subsequently, GFP⁺ cells were sorted and subjected to hypoxic treatment.

In Vitro Tube Formation Assay. Subconfluent pGIPZ control or CTCF-depleted MCF7 cells were switched to fresh serum-free ECM (Genlantis) with or without E2 (100 nM) or DP (100 μ M) for 24 h. The supernants were collected and diluted with fresh ECM for later use as conditioned media. The phenol red-free Matrigel (BD Biosciences) was thawed overnight at 4 °C. Two hundred microliters of Matrigel was added into each well in a prechilled 24-well plate. Matrigel was solidified by incubation at 37 °C for 1 h. Murine pulmonary endothelial cells (6×10^4 cells per well) were suspended in 500 μ L of serum-free ECM and seeded into each well. After 2 h of incubation, the culture media were changed to precollected conditioned media. The endothelial capillary-like network formation was photographed 2 and 12 h after treatment. To obtain quantitative readouts for the statistical analysis, all pictures were processed by the ImageJ program. From the processed images, total length of tubes and the number of endothelial outgrowth from each nodule were calculated.

Intradermal Angiogenesis. Intradermal angiogenesis was carried out as described (24). Briefly, control or CTCF-depleted MCF7 cells were suspended

and mixed with one drop of 0.4% (vol/vol) Trypan blue, which facilitated identification of the injection sites. The 5×10^4 cells were inoculated intradermally in a volume of 10 μ L on the ventral surface (preshaved) of SCID Beige female mice (Harlan). For estrogen treatment, each mouse was fed daily with 10 μ g E2 dissolved in sesame oil. Two days after injection, mice were killed and the skin flaps containing injection sites were carefully separated from the underlying muscle. The capillary density was quantified using a dissecting microscope. All vessels that touched the edge of the tumor inoculates were counted. The data represent mean value \pm SD. The procedures were performed in accordance with the institutional animal care and use committee of University of Florida.

In Vivo Electroporation of Retina. In vivo electroporation to transfect mouse retinal progenitors at P0 with plasmid DNA was performed as previously described (28). Newborn mouse pups were anesthetized by chilling on ice, and a small incision was made in the eyelid and sclera near the lens with a 30-gauge needle. Plasmid DNA solution in PBS (1.5 μ g/ μ L) was injected into the sub-retinal space through the incision by using a Hamilton syringe with a 33-gauge blunt-ended needle under a dissection microscope. Subsequently, electroporation was performed with tweezer-type electrodes (model 520, 7 mm in diameter; BTX) passing five 80-V pulses of 50-ms duration with 950-ms intervals using a pulse generator (ECM830 electroporator; BTX). This animal experiment was approved by the institutional animal care and use committee at Harvard University.

ACKNOWLEDGMENTS. We are grateful to Debabrata (Dev) Mukhopadhyay (Mayo Clinic) for the human VEGF promoter DNA. We thank Jorg Bungert and Suming Huang for critically reading the manuscript. This work was supported by grants from National Cancer Institute (R01CA137021), American Heart Association (0730219N), and Florida Bankhead-Coley Cancer Research Program (09BN-12-23092), to J.L., and the National Cancer Institute (R01CA089655) to D.W.S.

- Bergers G, Benjamin LE (2003) Tumorigenesis and the angiogenic switch. *Nat Rev Cancer* 3:401–410.
- Chung AS, Lee J, Ferrara N (2010) Targeting the tumour vasculature: Insights from physiological angiogenesis. *Nat Rev Cancer* 10:505–514.
- Ferrara N (2010) Vascular endothelial growth factor and age-related macular degeneration: From basic science to therapy. *Nat Med* 16:1107–1111.
- Carmeliet P, et al. (1996) Abnormal blood vessel development and lethality in embryos lacking a single VEGF allele. *Nature* 380:435–439.
- Ferrara N, et al. (1996) Heterozygous embryonic lethality induced by targeted inactivation of the VEGF gene. *Nature* 380:439–442.
- Ellis LM, Hicklin DJ (2008) VEGF-targeted therapy: Mechanisms of anti-tumour activity. *Nat Rev Cancer* 8:579–591.
- Hirota K, Semenza GL (2006) Regulation of angiogenesis by hypoxia-inducible factor 1. *Crit Rev Oncol Hematol* 59:15–26.
- Liao D, Johnson RS (2007) Hypoxia: A key regulator of angiogenesis in cancer. *Cancer Metastasis Rev* 26:281–290.
- Ferrara N (2004) Vascular endothelial growth factor: Basic science and clinical progress. *Endocr Rev* 25:581–611.
- Loureiro RM, D'Amore PA (2005) Transcriptional regulation of vascular endothelial growth factor in cancer. *Cytokine Growth Factor Rev* 16:77–89.
- Hyder SM (2006) Sex-steroid regulation of vascular endothelial growth factor in breast cancer. *Endocr Relat Cancer* 13:667–687.
- Gaszner M, Felsenfeld G (2006) Insulators: Exploiting transcriptional and epigenetic mechanisms. *Nat Rev Genet* 7:703–713.
- Phillips JE, Corces VG (2009) CTCF: Master weaver of the genome. *Cell* 137:1194–1211.
- Ohlsson R, Lobanenkov V, Klenova E (2010) Does CTCF mediate between nuclear organization and gene expression? *Bioessays* 32:37–50.
- Ao A, Wang H, Kamarajugadda S, Lu J (2008) Involvement of estrogen-related receptors in transcriptional response to hypoxia and growth of solid tumors. *Proc Natl Acad Sci USA* 105:7821–7826.
- Bao L, Zhou M, Cui Y (2008) CTCFBSDB: A CTCF-binding site database for characterization of vertebrate genomic insulators. *Nucleic Acids Res* 36(Database issue): D83–D87.
- Wendt KS, et al. (2008) Cohesin mediates transcriptional insulation by CCCTC-binding factor. *Nature* 451:796–801.
- Parelho V, et al. (2008) Cohesins functionally associate with CTCF on mammalian chromosome arms. *Cell* 132:422–433.
- Stedman W, et al. (2008) Cohesins localize with CTCF at the KSHV latency control region and at cellular c-myc and H19/Igf2 insulators. *EMBO J* 27:654–666.
- Rubio ED, et al. (2008) CTCF physically links cohesin to chromatin. *Proc Natl Acad Sci USA* 105:8309–8314.
- Recillas-Targa F, Bell AC, Felsenfeld G (1999) Positional enhancer-blocking activity of the chicken beta-globin insulator in transiently transfected cells. *Proc Natl Acad Sci USA* 96:14354–14359.
- Carroll JS, et al. (2006) Genome-wide analysis of estrogen receptor binding sites. *Nat Genet* 38:1289–1297.
- Welboren WJ, et al. (2009) CHIP-Seq of ERalpha and RNA polymerase II defines genes differentially responding to ligands. *EMBO J* 28:1418–1428.
- Shi W, Siemann DW (2002) Inhibition of renal cell carcinoma angiogenesis and growth by antisense oligonucleotides targeting vascular endothelial growth factor. *Br J Cancer* 87:119–126.
- Filippova GN, et al. (2002) Tumor-associated zinc finger mutations in the CTCF transcription factor selectively alter its DNA-binding specificity. *Cancer Res* 62:48–52.
- Stahl A, et al. (2010) The mouse retina as an angiogenesis model. *Invest Ophthalmol Vis Sci* 51:2813–2826.
- Gariano RF, Gardner TW (2005) Retinal angiogenesis in development and disease. *Nature* 438:960–966.
- Matsuda T, Cepko CL (2004) Electroporation and RNA interference in the rodent retina in vivo and in vitro. *Proc Natl Acad Sci USA* 101:16–22.
- Okamoto N, et al. (1997) Transgenic mice with increased expression of vascular endothelial growth factor in the retina: A new model of intraretinal and subretinal neovascularization. *Am J Pathol* 151:281–291.
- Scott KC, Taubman AD, Geyer PK (1999) Enhancer blocking by the Drosophila gypsy insulator depends upon insulator anatomy and enhancer strength. *Genetics* 153: 787–798.
- Green AR, et al. (2009) Loss of expression of chromosome 16q genes DPEP1 and CTCF in lobular carcinoma in situ of the breast. *Breast Cancer Res Treat* 113:59–66.
- Rakha EA, Pinder SE, Paish CE, Ellis IO (2004) Expression of the transcription factor CTCF in invasive breast cancer: A candidate gene located at 16q22.1. *Br J Cancer* 91: 1591–1596.
- Filippova GN, et al. (1998) A widely expressed transcription factor with multiple DNA sequence specificity, CTCF, is localized at chromosome segment 16q22.1 within one of the smallest regions of overlap for common deletions in breast and prostate cancers. *Genes Chromosomes Cancer* 22:26–36.
- Lin T, Ponn A, Hu X, Law BK, Lu J (2010) Requirement of the histone demethylase LSD1 in Snai1-mediated transcriptional repression during epithelial-mesenchymal transition. *Oncogene* 29:4896–4904.